Journal of Power Sources 199 (2012) 278–286

Contents lists available at SciVerse ScienceDirect

Journal of Power Sources

journal homepage: www.elsevier.com/locate/jpowsour

Synthesis of Li_2FeSiO_4/C nanocomposite cathodes for lithium batteries by a novel synthesis route and their electrochemical properties

Bin Shao, Izumi Taniguchi*

Department of Chemical Engineering, Graduate School of Science and Engineering, Tokyo Institute of Technology, 12-1, Ookayama-2, Meguro-ku, Tokyo 152-8552, Japan

ARTICLE INFO

Article history:
Received 23 May 2011
Received in revised form 29 August 2011
Accepted 13 October 2011
Available online 20 October 2011

Keywords:
Li_2FeSiO_4
Spray pyrolysis
Lithium-ion batteries
Cathode
Nanocomposite

ABSTRACT

Li_2FeSiO_4/C nanocomposites were synthesized by a novel synthesis route, i.e., a combination of spray pyrolysis and wet ball-milling followed by annealing. The effect of process parameters such as spray pyrolysis temperature, ball-milling time, carbon content in the wet ball-milling process and annealing temperature on the physical and electrochemical properties of Li_2FeSiO_4/C nanocomposites was investigated. The final sample was identified as Li_2FeSiO_4 with a $P2_1$ monoclinic structure by X-ray diffraction analysis. Field-emission scanning electron microscopy and transmission electron microscopy with energy-dispersive spectroscopy verified that the Li_2FeSiO_4/C nanocomposites are agglomerates of Li_2FeSiO_4 primary particles with a geometric mean diameter of 65 nm and that the carbon was well-distributed on the surface of the agglomerates. A Li_2FeSiO_4/C nanocomposite sample was used as an electrode material for rechargeable lithium batteries, and electrochemical measurements were carried out by using Li|1 M $LiPF_6$ in EC: DMC = 1:1| Li_2FeSiO_4/C cells at room temperature. The Li_2FeSiO_4/C nanocomposite electrode delivered a first discharge capacity of 154 mAh g^{-1} at 0.05 C, corresponding to 93% of the theoretical value. Furthermore, the cycleability and rate capability of the cells were good.

1. Introduction

The demand for large-scale lithium-ion batteries in electric vehicles (EVs), emergency power systems and dispersed electric power sources has led to the research and development of inexpensive, high-safety and long-lifetime cathode materials [1]. Currently, commercial lithium-ion batteries mostly rely on lithium transition-metal oxides, such as $LiCoO_2$, $LiNiO_2$ and $LiMn_2O_4$. However, some issues including the high cost and toxicity of Co, exothermic oxidation reaction between the organic electrolyte and highly oxidized transition metal elements [2–7] prevent these oxide materials from being used as large-scale lithium battery cathode. Therefore, considerable effort has been made to find alternative cathode materials for lithium-ion batteries.

Padhi et al. [8] reported that the polyanionic material $LiFePO_4$ can be used as a cathode material of lithium-ion batteries with stable cycleability and high thermal stability. However, the low electronic and ionic conductivities of $LiFePO_4$ [2–5] prevent it from further application. The development of synthesis processes to prepare nanostructured materials containing carbon or carbon nanocomposites has now successfully overcome these problems [9].

With this background, some researchers have attempted to develop new polyoxyanionic materials with higher energy density and lower cost. Nytén et al. [10] first synthesized Li_2FeSiO_4 and showed the possibility of using Li_2FeSiO_4 as an active cathode material in lithium batteries. Li_2FeSiO_4 also suffers from poor electronic conductivity [11], which is five orders of magnitude lower than that of $LiFePO_4$. However, it includes Si and Fe elements which are in plentiful apply and a stable Fe–Si–O bond which provides high thermal stability. Moreover, Li_2FeSiO_4 enables the possibility of extraction more than one lithium per molecule [5,12]. Thus, many researchers are still attempting to enhance the electrochemical properties of Li_2FeSiO_4 by investigating various synthesis methods, such as the solid-state reaction method [10,13,14], sol–gel method [11,15–17], hydrothermal synthesis [11,17], microwave-solvothermal synthesis [5] and sol–gel-assisted hydrothermal synthesis [18]. However, the solid-state reaction method requires prolonged heat treatment at a high temperature. The sol–gel method involves multistep operations and requires a long reaction time. In particular, the necessity of evaporating a large amount of solvent at a low temperature makes it difficult to use the sol–gel method in large scale applications. Hydrothermal synthesis requires starting materials containing excess Li, and several days are needed to synthesize Li_2FeSiO_4. Thus, a more effective synthesis route for obtaining Li_2FeSiO_4 with excellent electrochemical performance is desirable.

* Corresponding author. Tel.: +81 3 5734 2155; fax: +81 3 5734 2155.
E-mail address: taniguchi.i.aa@m.titech.ac.jp (I. Taniguchi).

0378-7753/$ – see front matter © 2011 Elsevier B.V. All rights reserved.
doi:10.1016/j.jpowsour.2011.10.050

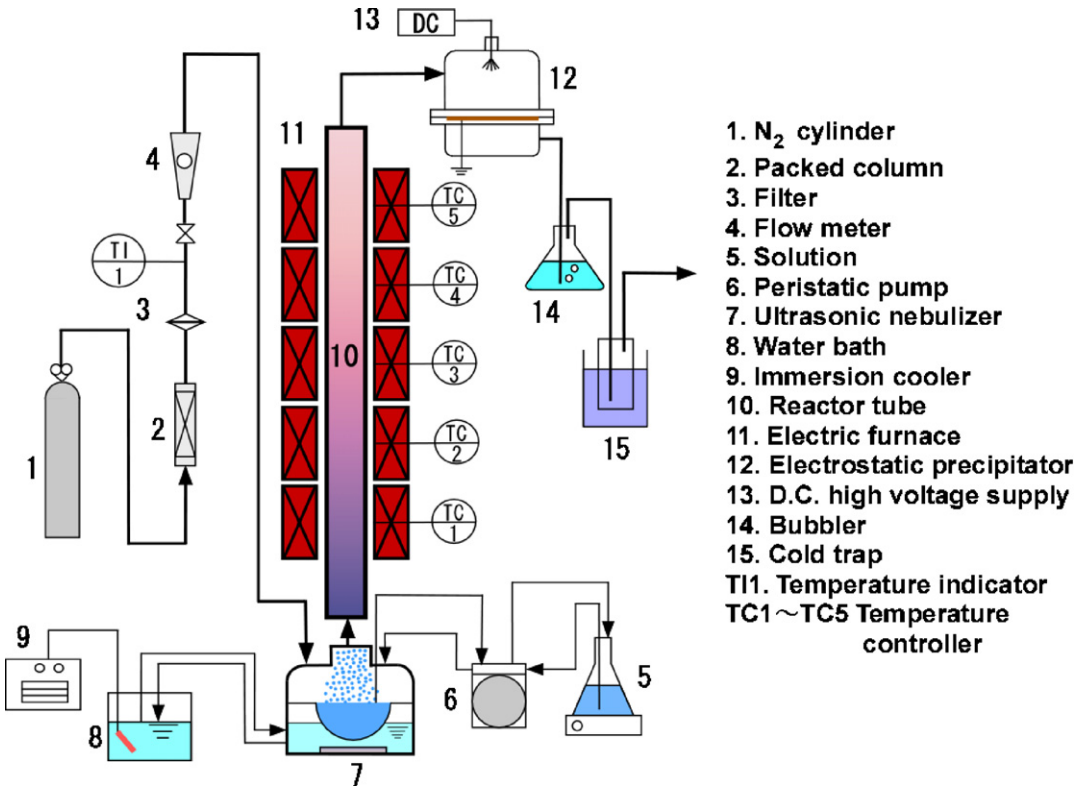

Fig. 1. Schematic diagram of the experimental apparatus for SP.

Spray pyrolysis (SP) is a continuous method for preparing fine ceramic powders with a uniform chemical composition and a narrow particle size distribution from the micrometer order to the submicrometer order and can be easily used for large-scale applications [19]. Moreover, it is possible to use SP at a low reactor temperature to prepare amorphous Li_2FeSiO_4 particles with a uniform particle size distribution and chemical composition. Thus, it can be expected from our previous work [20] that Li_2FeSiO_4/C nanocomposites can be synthesized by a combination of SP and ball-milling followed by heat treatment.

In this study, a combination of SP and wet ball-milling (WBM) followed by annealing was used to prepare Li_2FeSiO_4/C nanocomposites from precursors of $LiNO_3$, $Fe(NO_3)_3{\cdot}9H_2O$ and tetraethylorthosilicate (TEOS). The effect of process parameters such as SP temperature, ball-milling time, carbon content in the WBM process and annealing temperature on the physical and electrochemical properties of Li_2FeSiO_4/C nanocomposites was investigated.

2. Experimental

2.1. Precursor solution

The precursor solution was prepared by dissolving stoichiometric amounts of $LiNO_3$ (98% purity), $Fe(NO_3)_3{\cdot}9H_2O$ (98% purity) and TEOS (99% purity) in distilled water. To hydrolyze the TEOS, several droplets of HNO_3 were added to the precursor solution. All chemicals were purchased from Wako Pure Chemical Industries Ltd., Japan.

2.2. Experimental setup and procedure

Fig. 1 shows a schematic diagram of the spray pyrolysis system. It mainly consists of a droplet generator, a laminar flow aerosol reactor and a particle collector. The droplet generator comprises an ultrasonic nebulizer (7), a peristaltic pump (6) for supplying the precursor solution (5) to the ultrasonic nebulizer and a thermostat circulation system (8, 9). The laminar flow aerosol reactor (10) used in the present study is a high-quality quartz tube of 70 mm inner diameter and 1.5 m length, which is inserted into a vertical electric furnace (11). The particle collector is an electrostatic precipitator (12), which consists of a glass chamber, tungsten wire electrodes and a grounded plate electrode with a glass collection plate on its top. A d.c. high voltage was applied to the tungsten wire electrodes.

The precursor solution was atomized at a frequency of 1.7 MHz by the ultrasonic nebulizer. The sprayed droplets were transported to the reactor by N_2 gas with a flow rate of 2 $dm^3\ min^{-1}$, then heated from 300 to 700 °C by the electric furnace, and converted into solid particles through the evaporation of the solvent, the precipitation of the solute, drying, thermal decomposition and annealing within the laminar flow aerosol reactor. The resulting powders were collected at the reactor exit by the electrostatic precipitator, which operated at 150 °C, while the gases were dried and cleaned by passing them through a bubbler (14) and a cold trap (15).

The samples prepared at various SP temperatures from 300 to 700 °C were milled with acetylene black (AB, electrical conductivity of 500 S m^{-1}, specific surface area of 68 $m^2\ g^{-1}$) in ethanol by planetary high-energy ball-milling (Fritsch, Pulverisette 7), and then annealed at temperatures from 500 to 800 °C for 4 h in a N_2 + 3% H_2 or N_2 atmosphere. To investigate the effect of the WBM process conditions on the physical and electrochemical properties of Li_2FeSiO_4/C nanocomposites, the samples prepared by SP were ball-milled for various times ranging from 1 to 6 h with the AB content ranging from 5 to 20 wt.%. Fig. 2 shows a flowchart for the preparation of Li_2FeSiO_4/C nanocomposites.

For the preparation of Li_2FeSiO_4, the samples prepared at various SP temperatures from 300 to 700 °C were then annealed at temperatures from 500 to 700 °C for 4 h in a N_2 + 3% H_2 atmosphere.

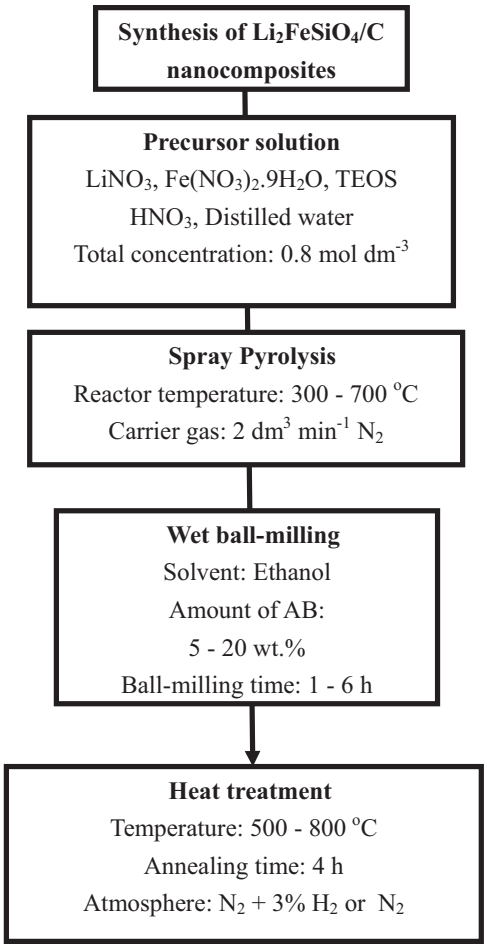

Fig. 2. Flowchart of the preparation of Li_2FeSiO_4/C nanocomposites.

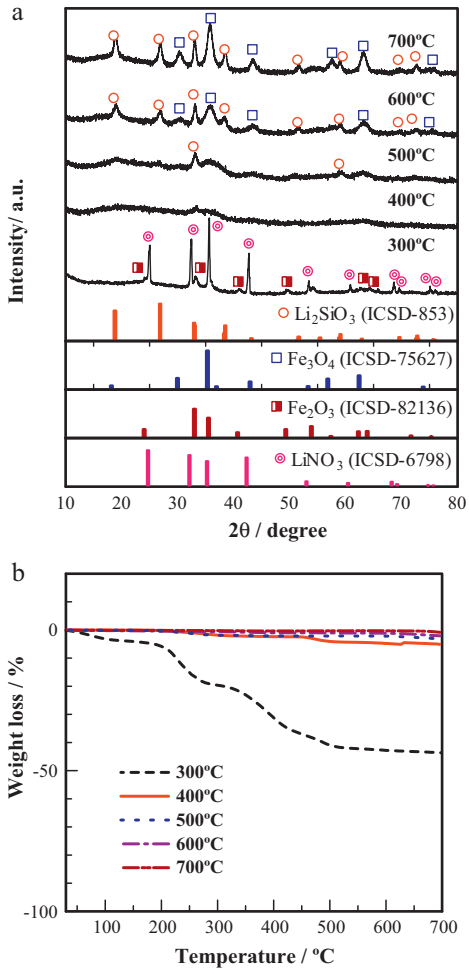

Fig. 3. (a) XRD patterns and (b) thermogravimetry curves of the samples prepared at temperatures from 300 to 700 °C by SP.

2.3. Physical characterization

The thermal decomposition behavior of the SP samples was determined by a Rigaku Thermo Plus thermogravimetry (TG) and differential thermal analysis (DTA) 8120 apparatus at a heating rate of 10 °C min^{-1} and a flow rate of 150 ml min^{-1} in a dry He atmosphere. The samples were heated from room temperature to 700 °C. The crystalline phase of the samples was studied by X-ray diffraction (XRD, Rigaku, Ultima IV with D/teX Ultra) analysis with Cu-Kα radiation. The surface morphology of the samples was examined by field-emission scanning electron microscopy (FE-SEM, Hitachi, S4500) or SEM (Keyence YE-8800) at 8 kV. The measurements and calculation of the particle size distribution, geometric mean diameter, $d_{p,g}$, and geometric standard deviation, σ_g, are described elsewhere [19]. The interior structure of the Li_2FeSiO_4/C nanocomposite particles was observed by transmission electron microscopy (TEM, JEOL Ltd., JEM-2010F) with energy-dispersive spectroscopy (EDS). The carbon content of the Li_2FeSiO_4/C nanocomposites was determined using an element analyzer (Yanaco, CHN Corder MT-6).

2.4. Electrochemical measurements

Electrochemical characterization was performed by assembling a CR2032 coin cell for galvanostatic charge–discharge testing. The cell comprised a lithium metal negative electrode and a Li_2FeSiO_4/C composite positive electrode that were separated by a microporous polypropylene film. A 1 mol dm^{-3} solution of $LiPF_6$ in a mixed solvent of ethylene carbonate (EC) and dimethyl carbonate (DMC) with 1:1 volume ratio (Tomiyama Pure Chemical Co., Ltd.) was used as the electrolyte. The cathode consisted of 70 wt.% Li_2FeSiO_4, 10 wt.% polyvinylidene fluoride (PVdF) as a binder and 20 wt.% AB, which included the AB in the Li_2FeSiO_4/C nanocomposites. These materials were dispersed in 1-methyl-2-pyrrolidinone (NMP). The resultant slurry was spread uniformly onto an aluminum foil using the doctor blade technique, and the coated aluminum foil was then dried in a vacuum oven for 6 h at 110 °C. The cathode was punched into circular discs and then scraped in order to standardize the area of the cathode (1 cm^2). The cell was assembled inside a glove box filled with high-purity argon gas (99.9995% purity). The cells were tested galvanostatically between 1.5 and 4.8 V versus Li^+/Li on multi-channel battery testers (Hokuto Denko, HJ1010mSM8A) at different charge–discharge rates from 0.05 to 2 C (1 C = 166 mAh g^{-1}). Current densities and specific capacities were calculated on the basis of the mass of Li_2FeSiO_4 in the cathode. All electrochemical measurements were performed at room temperature.

3. Results and discussion

3.1. Preparation of Li_2FeSiO_4

XRD patterns of the samples prepared at SP temperatures from 300 to 700 °C are shown in Fig. 3a. The diffraction peaks of the sample prepared at 300 °C were attributed to $LiNO_3$ (ICSD – 6798) and Fe_2O_3 (ICSD – 82136). However, no peak corresponding to a

Si compound was detected. The samples prepared at 400 and 500 °C were almost amorphous, and $LiNO_3$, $Fe(NO_3)_3 \cdot 9H_2O$ and TEOS were perfectly decomposed during the SP process, which was also confirmed by the thermal decomposition analysis of the as-prepared samples, as shown in Fig. 3b. The XRD peaks of the samples prepared at 600 and 700 °C were attributed to Li_2SiO_3 (ICSD – 853) and Fe_3O_4 (ICSD – 75627). As a result, no desired peak was detected from the samples as-prepared by SP. However, from these results, it was predicted that Li_2FeSiO_4 would be formed from additional annealing of the as-prepared samples in a reductive atmosphere, in which the Fe^{3+} in Fe_3O_4 should be reduced to Fe^{2+} and react with Li_2SiO_3. To test this prediction, the samples prepared by SP at 400 °C were then annealed at various temperatures from 500 to 700 °C for 4 h in a 3% $H_2 + N_2$ atmosphere. The XRD patterns of the annealed samples are shown in Fig. 4. While the XRD peaks of the sample annealed at 500 °C were attributed to Li_2SiO_3 and Fe_3O_4, those of the sample annealed at 600 °C were clearly identified as the Li_2FeSiO_4 phase with the space group $P2_1$ from the results reported by Nishimura et al. [21]. However some impurity peaks corresponding to Fe (ICSD – 52258) and Li_2SiO_3 were also detected in the sample annealed at 700 °C. This may explain why the rate of reaction for the reduction of the Fe^{3+} in Fe_3O_4 was so high at an annealing temperature of 700 °C that Fe was formed before the reaction between FeO and Li_2SiO_3.

Fig. 5 shows SEM images of the samples prepared at 400 °C by SP with and without annealing at 600 °C for 4 h in a 3% $H_2 + N_2$ atmosphere. The as-prepared powders are spherical with a geometric mean diameter of 0.75 μm and a standard deviation of 1.4 (Fig. 5a). There is no significant change in morphology after annealing and a slight decrease in particle size due to the crystallization of amorphous powders can be seen in Fig. 5b.

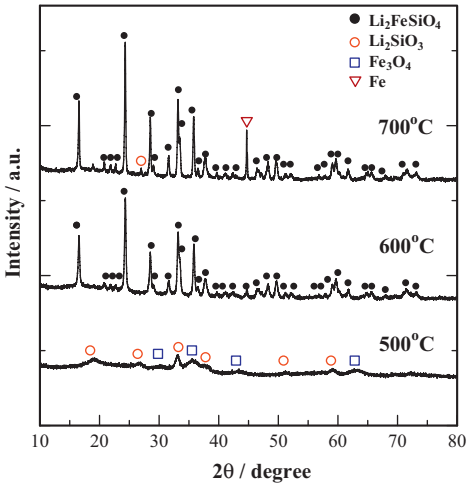

Fig. 4. XRD patterns of the samples prepared by SP followed by annealing at 500, 600 and 700 °C in a 3% $H_2 + N_2$ atmosphere.

The Li_2FeSiO_4 samples that were prepared at 400 °C by SP and then annealed at 600 °C for 4 h in a 3% $H_2 + N_2$ atmosphere were used as cathode materials for rechargeable lithium batteries, and electrochemical measurements were carried out by using Li|1 M $LiPF_6$ in EC: DMC = 1:1| Li_2FeSiO_4 cells at room temperature.

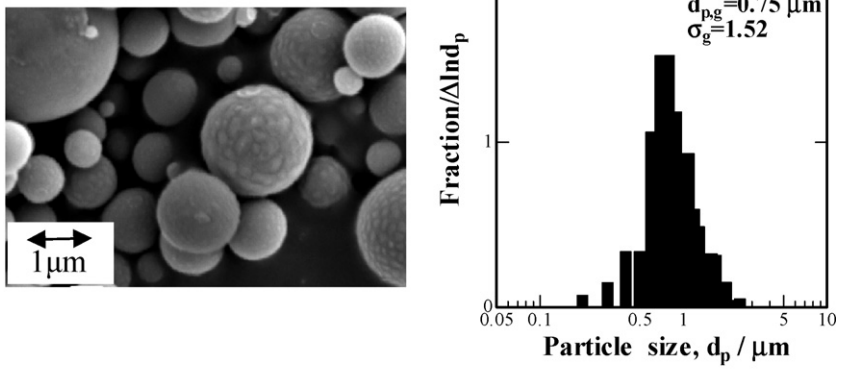

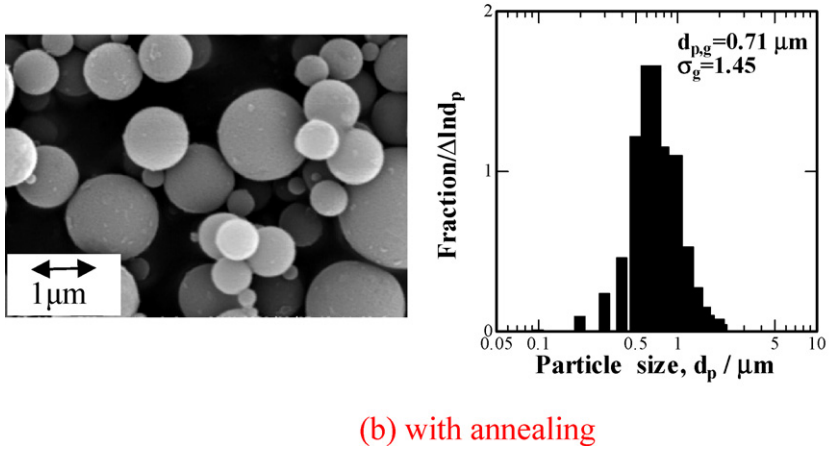

Fig. 5. SEM images and particle size distributions of the samples prepared at 400 °C by SP (a) without and (b) with annealing at 600 °C in a 3% $H_2 + N_2$ atmosphere.

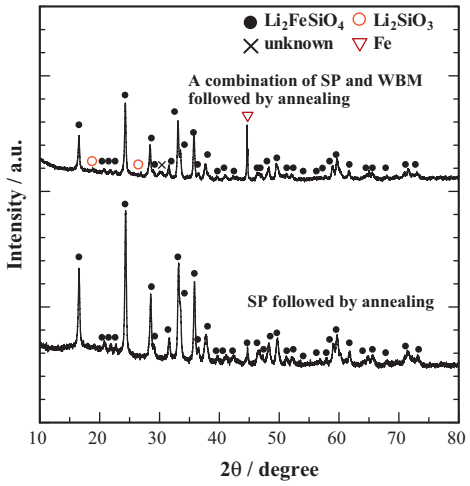

Fig. 6. XRD patterns of the samples prepared by a combination of SP at 400 °C and WBM followed by annealing at 600 °C in a 3% $H_2 + N_2$ atmosphere. Carbon content in WBM process: 20 wt.%. Ball-milling time: 4 h.

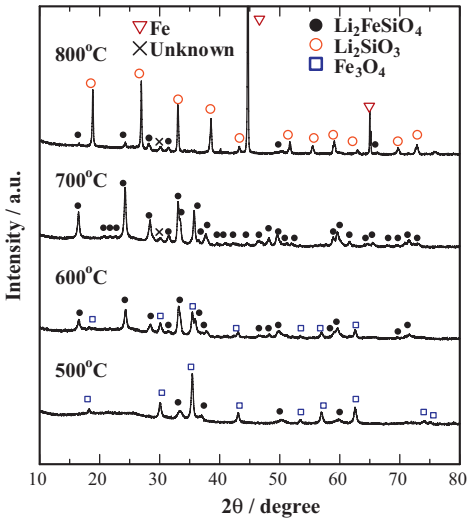

Fig. 7. XRD patterns of the samples prepared by a combination of SP at 400 °C and WBM followed by annealing at temperatures from 500 to 800 °C in a N_2 atmosphere. Carbon content in WBM process: 20 wt.%. Ball-milling time: 4 h.

However, the cells did not operate as rechargeable lithium batteries, which might have been due to their poor electronic conductivity and relatively large particle size.

3.2. Preparation of Li_2FeSiO_4/C nanocomposites

To enhance the electrochemical properties of Li_2FeSiO_4, the preparation of Li_2FeSiO_4/C nanocomposites was attempted by a novel synthesis route, i.e., a combination of SP and WBM followed by annealing. The amorphous Li_2FeSiO_4 sample prepared at 400 °C by SP was chosen as the precursor material for the WBM procedure.

Fig. 6 shows the XRD patterns of the samples prepared by a combination of SP and WBM for 4 h with heat treatment at 600 °C in a 3% $H_2 + N_2$ atmosphere. The carbon content was 20 wt.% in the WBM process. For comparison, the XRD patterns of the sample prepared by SP with heat treatment at 600 °C in the same atmosphere are also shown in the figure. The XRD peaks of the present sample were identified as the Li_2FeSiO_4 phase with the space group $P2_1$. The Fe phase was also clearly detected at $2\theta = 45°$. However, the sample prepared by SP with heat treatment was indexed to only the desired phase. This may indicate that the addition of carbon increases the strength of the reducing condition in the annealing procedure. As a result, the Fe phase was detected in the XRD patterns owing to the conversion of Fe_3O_4 to Fe in the strongly reducing atmosphere. Thus, the samples after WBM were annealed at temperatures from 500 to 800 °C in a N_2 atmosphere. The XRD patterns of these samples are shown in Fig. 7. As can be seen, Li_2FeSiO_4/C nanocomposites were successfully prepared by a combination of SP and WBM followed by heat treatment at 700 °C in a N_2 atmosphere, although an unidentified peak was observed at $2\theta = 30°$.

3.3. Effect of ball-milling time on physical and electrochemical properties of Li_2FeSiO_4/C nanocomposites

Fig. 8 shows the XRD patterns of the final samples prepared by the present method with ball-milling times ranging from 1 to 6 h. The carbon content was 20 wt.% in the WBM process. The XRD data for all samples were indexed to the Li_2FeSiO_4 phase with the space group $P2_1$. However, Fe was clearly detected as an impurity in the final sample prepared with a ball-milling time of 6 h. Furthermore, the peak intensity slightly decreased with increasing ball-milling time. This may indicate that the primary particle size of the present sample decreases with increasing ball-milling time.

The morphology and interior structure of the final samples prepared with ball-milling times of 1 and 4 h were observed by FE-SEM and by TEM with EDS analysis. The results are shown in Fig. 9a and b. With increasing ball-milling time from 1 to 4 h, the geometric mean diameter of the primary particles was reduced from 105 to 65 nm. Furthermore, it was clarified by the TEM observation with EDS analysis that the final sample prepared with a ball-milling time of 4 h is a well-mixed Li_2FeSiO_4/C nanocomposite, compared with the sample prepared with a ball-milling time of 1 h.

Galvanostatic charge–discharge measurements were carried out with lithium cells at a rate of 0.1 C to investigate the effect of ball-milling time on the electrochemical properties of the Li_2FeSiO_4/C nanocomposite cathodes. Fig. 10 shows the first charge–discharge profiles of the Li_2FeSiO_4/C nanocomposites prepared with various ball-milling times. The first discharge capacity of the Li_2FeSiO_4/C nanocomposite increases with ball-milling time up to 4 h, reaching a maximum value of 148 mAh g^{-1}, which corresponds to 89% of the theoretical value of 166 mAh g^{-1}. This may be due to the fact that for a longer ball-milling time of 4 h, the particle

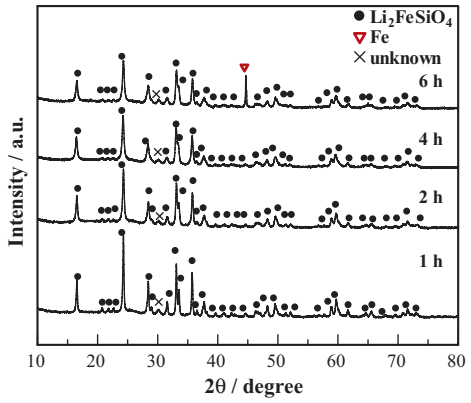

Fig. 8. XRD patterns of the final samples prepared by the present method with ball-milling times from 1 to 6 h. Annealing temperature: 700 °C. Carbon content in WBM process: 20 wt.%. Annealing atmosphere: N_2.

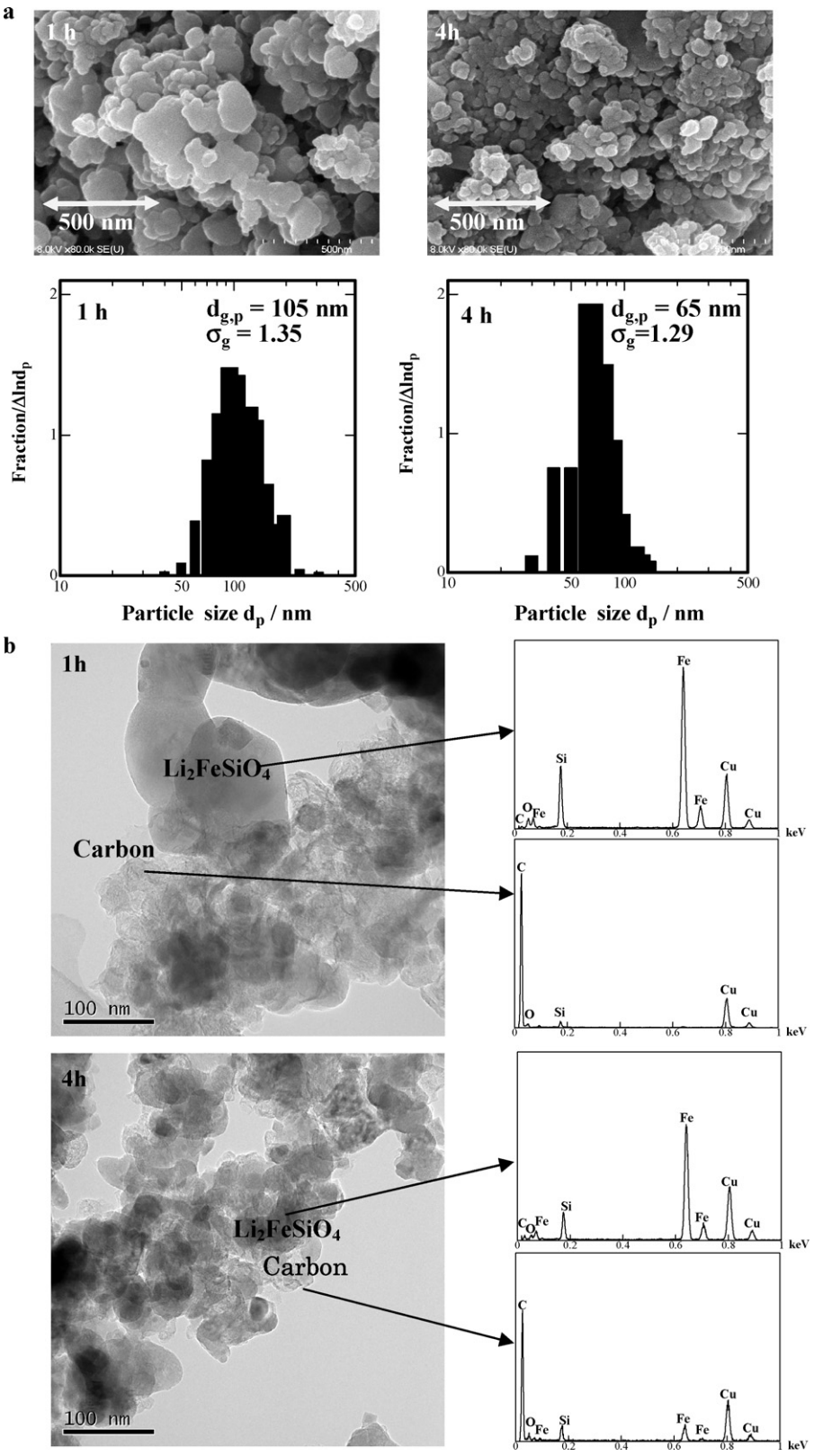

Fig. 9. (a) SEM images and primary particle size distribution, and (b) TEM images and EDS spectra of Li_2FeSiO_4/C nanocomposites prepared by a combination of SP at 400 °C and WBM with ball-milling times of 1 and 4 h followed by annealing at 700 °C in a N_2 atmosphere. Carbon content in WBM process: 20 wt.%.

size was smaller and the carbon was better distributed between the Li_2FeSiO_4 particles, as shown in Fig. 9b. The smaller primary particle size may have reduced the diffusion pathway of lithium ions within the bulk material, thus enhancing the electrochemical performance of the cathode. On the other hand, a further increase in the ball-milling time resulted in the discharge capacity slightly decreasing owing to the formation of the impurity phase (Fe), as shown in Fig. 8.

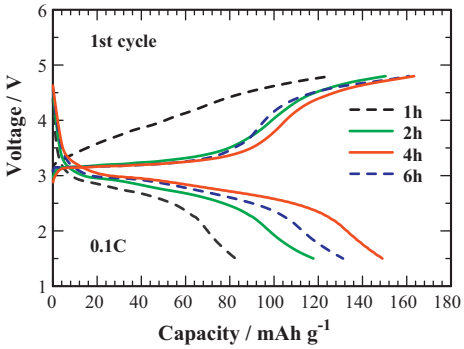

Fig. 10. First charge–discharge profiles of the cells containing Li_2FeSiO_4/C nanocomposites prepared by a combination of SP at 400 °C and WBM with ball-milling times from 1 to 6 h followed by annealing at 700 °C in a N_2 atmosphere. Carbon content in WBM process: 20 wt.%.

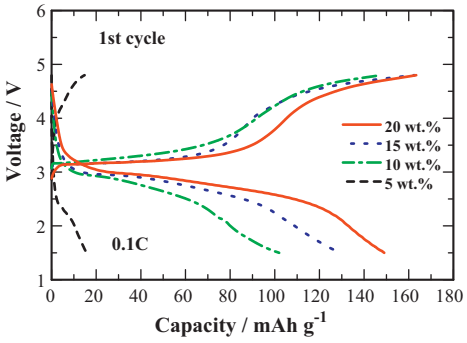

Fig. 12. First charge–discharge profiles of Li_2FeSiO_4/C nanocomposites prepared by a combination of SP at 400 °C and WBM with carbon contents from 5 to 20 wt.% followed by annealing at 700 °C in a N_2 atmosphere. Ball-milling time: 4 h.

3.4. *Effect of carbon content in WBM process on physical and electrochemical properties of Li_2FeSiO_4/C nanocomposites*

Li_2FeSiO_4/C nanocomposites were prepared by the present method with carbon contents of 10 and 20 wt.% in the WBM process, and the surface morphology and interior structure of the samples were then examined by SEM and by TEM with EDS analysis. Fig. 11 shows the results. In the sample prepared with a carbon content of 10 wt.% in the WBM process, larger primary particles aggregated with each other to form larger Li_2FeSiO_4 secondary particles. On the other hand, the sample prepared with a carbon content of 20 wt.% in the WBM process consisted of smaller primary particles, and soft agglomerates were formed. This indicates that the smaller amount of carbon additive had a greater effect on enhancing the growth of Li_2FeSiO_4 primary particles in the annealing process.

The effect of the carbon content in the WBM process on the electrochemical properties of Li_2FeSiO_4/C nanocomposites was investigated at a galvanostatic charge–discharge rate of 0.1 C, as shown in Fig. 12. The Li_2FeSiO_4/C nanocomposite cathodes delivered first discharge capacities of 16, 102, 130 and 145 mAh g^{-1} for carbon contents of 5, 10, 15 and 20 wt.%, respectively. An increase in the carbon content enhances the electrochemical performance of the Li_2FeSiO_4/C nanocomposite cathode. In particular, the discharge capacity exhibits a marked increase when the carbon content is increased to 10 wt.%. This shows that the carbon

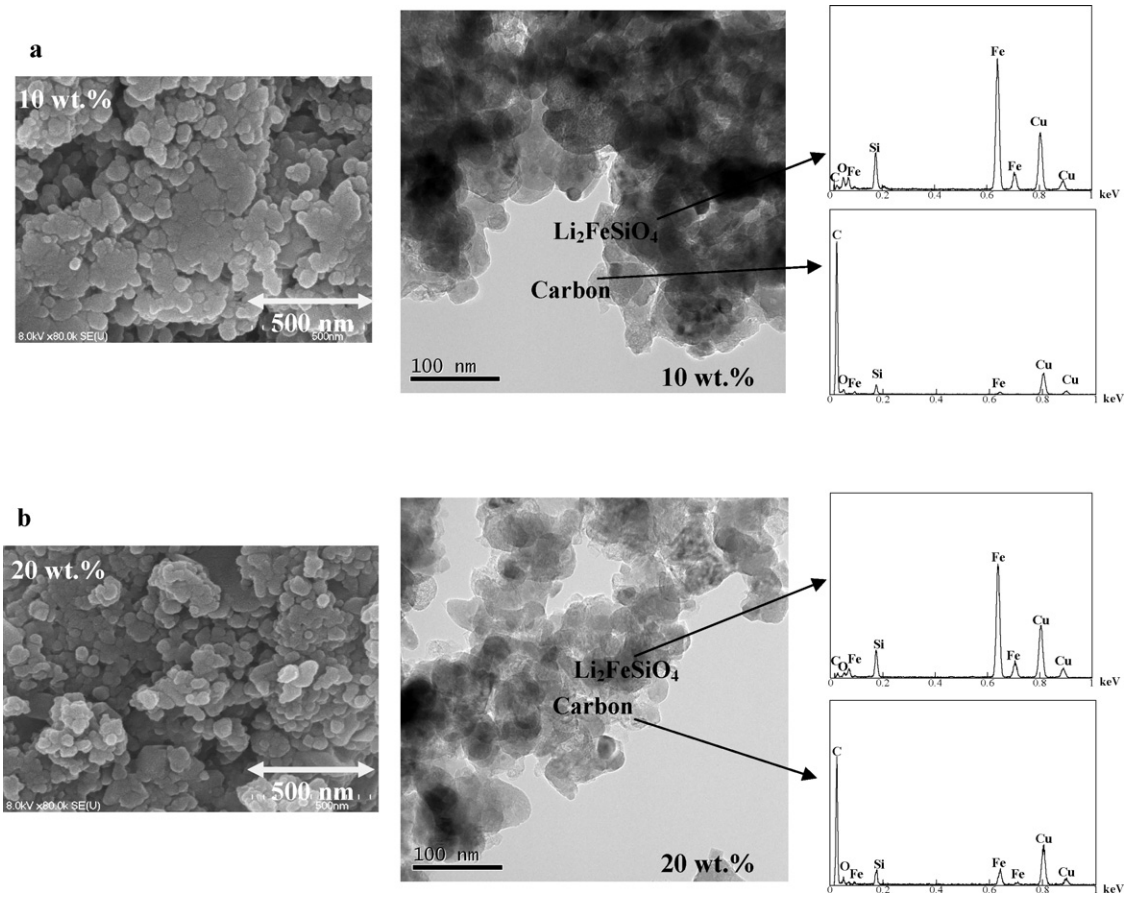

Fig. 11. SEM and TEM images and EDS spectra of Li_2FeSiO_4/C nanocomposites prepared by a combination of SP at 400 °C and WBM followed by annealing at 700 °C in a N_2 atmosphere. Ball-milling time: 4 h. (a) Carbon content in WBM process: 10 wt.%. (b) Carbon content in WBM process: 20 wt.%.

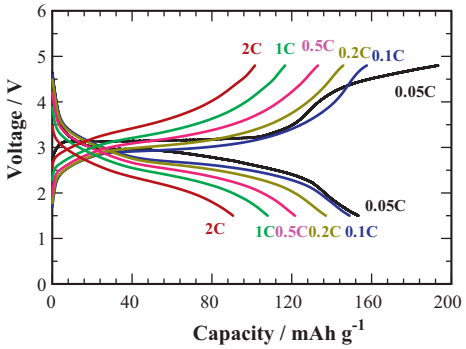

Fig. 13. Charge–discharge profiles of the Li_2FeSiO_4/C nanocomposites at various charge–discharge rates.

additive added to Li_2FeSiO_4 in the WBM process plays key role in the enhancing the electrochemical properties of Li_2FeSiO_4.

3.5. Cycleability and rate capability of Li_2FeSiO_4/C nanocomposite cathode

In the previous sections, it was shown that the Li_2FeSiO_4/C nanocomposite with the best electrochemical performance was prepared by a combination of SP at 400 °C and WBM with a ball-milling time of 4 h and a carbon content of 20 wt.% followed by annealing at 700 °C for 4 h in a N_2 atmosphere. Thus, further electrochemical investigations were carried out on this material.

A cycle performance of cells containing the above Li_2FeSiO_4/C nanocomposite was tested at charge–discharge rates from 0.05 to 2 C, in which 10 cycles were carried out at each rate. Then the charge–discharge rate was reduced to 0.1 C for the final 10 cycles. The first charge–discharge profiles of the cells containing Li_2FeSiO_4/C nanocomposites for each 10 cycles are presented in Fig. 13. At a charge–discharge rate of 0.05 C, the cell delivers a discharge capacity of 154 mAh g^{-1}, which corresponds to 93% of the theoretical capacity, and a small irreversible capacity. The cells also exhibit first discharge capacities of 148 mAh g^{-1} at 0.1 C, 138 mAh g^{-1} at 0.2 C, 123 mAh g^{-1} at 0.5 C, 110 mAh g^{-1} at 1 C and 91 mAh g^{-1} at 2 C.

Fig. 14 shows the cycle performance of the Li_2FeSiO_4/C nanocomposite cathodes. After 70 cycles the cell delivers a discharge capacity of 144 mAh g^{-1} at 0.1 C, which indicates a little capacity fading in comparison with the value of the 1st cycle (149 mAh g^{-1}). Furthermore, the capacity retention is 94% after 100 cycles at a constant charge–discharge rate of 0.1 C (see the inset). These results can be attributed to the well-distributed carbon, which acts as an electronic conductor. The high purity, nanometer particle size ($d_{g,p}$ = 65 nm) and narrow particle size distribution (σ_g = 1.29), together with the well-distributed carbon, result in the excellent electrochemical performance of the Li_2FeSiO_4/C nanocomposite cathode. The good electrochemical performance, together with the low cost and toxicity, makes the Li_2FeSiO_4/C nanocomposite cathode material a promising candidate for large-scale lithium-ion batteries. Furthermore, the proposed novel synthesis route, i.e., a combination of SP and WBM followed by annealing, is effective for reducing the annealing time at a high temperature. As a result, the cost of producing Li_2FeSiO_4/C nanocomposites by this method is expected to be lower than that of conventional preparation technique.

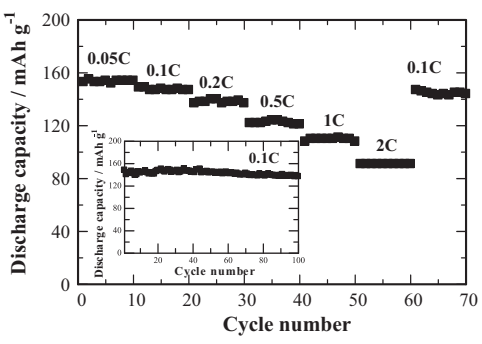

Fig. 14. Cycle performance of Li_2FeSiO_4/C nanocomposite cathodes.

4. Conclusions

A novel preparation route, i.e., a combination of SP and WBM followed by annealing, was developed to prepare Li_2FeSiO_4/C nanocomposites as a cathode material for lithium batteries. The effect of process parameters such as SP temperature, ball-milling time and carbon content in the WBM process and the annealing temperature on the physical and electrochemical properties of the Li_2FeSiO_4/C nanocomposites was discussed. The obtained Li_2FeSiO_4/C nanocomposites had a monoclinic structure with the space group $P2_1$. The Li_2FeSiO_4/C nanocomposite with the best electrochemical performance was prepared by a combination of SP at 400 °C and WBM with a ball-milling time of 4 h and a carbon content of 20 wt.% followed by annealing at 700 °C for 4 h in a N_2 atmosphere. This material consisted of agglomerates of Li_2FeSiO_4 primary particles with a geometric mean diameter of 65 nm, and the carbon was well distributed on the surface of the agglomerates. The Li_2FeSiO_4/C nanocomposite sample was used as an electrode material for rechargeable lithium batteries, and electrochemical measurements were carried out by using Li|1 M $LiPF_6$ in EC: DMC = 1:1| Li_2FeSiO_4/C cells at room temperature. The Li_2FeSiO_4/C nanocomposite electrode delivered a first discharge capacity of 154 mAh g^{-1} at 0.05 C, corresponding to 93% of the theoretical value, and the cycleability and rate capability of the cells were high, which might have been due to the high purity of Li_2FeSiO_4 phase, nanometer particle size ($d_{g,p}$ = 65 nm) and the narrow particle size distribution (σ_g = 1.29), together with the well-distributed carbon. The results of this study indicate that Li_2FeSiO_4/C nanocomposites are good candidates for use as the cathode material of large-scale lithium batteries.

Acknowledgements

The authors are grateful to Mr. A. Hori and Mr. J. Koki, staff members of the Center for Advanced Materials Analysis (Tokyo Institute of Technology, Japan) for the FE-SEM and TEM observations of the samples.

References

[1] J.B. Goodenough, Y. Kim, Chem. Mater. 22 (2010) 587–603.
[2] J.M. Tarascon, M. Armand, Nature 414 (2001) 359–367.
[3] M.S. Whittingham, Chem. Rev. 104 (2004) 4271–4310.
[4] J.W. Fergus, J. Power Sources 195 (2010) 939–954.
[5] T. Muraliganth, K.R. Stroukoff, A. Manthiram, Chem. Mater. 22 (2010) 5754–5761.
[6] P.G. Balakrishnan, R. Ramesh, T. Prem Kumar, J. Power Sources 155 (2006) 401–414.
[7] D.D. MacNeil, Z.H. Lu, Z.H. Chen, J.R. Dahn, J. Power Sources 108 (2002) 8–14.
[8] A.K. Padhi, K.S. Nanjundaswamy, J.B. Goodenough, J. Electrochem. Soc. 144 (1997) 1188–1194.
[9] D. Jugović, D. Uskoković, J. Power Sources 190 (2009) 538–544.
[10] A. Nytén, A. Abouimrane, M. Arman, T. Gustafsson, J.O. Thomas, Electrochem. Commun. 7 (2005) 156–160.
[11] R. Dominko, J. Power Sources 184 (2008) 462–468.
[12] Z.L. Gong, Y.X. Li, Y. Yang, Electrochem, Solid-State Lett. 9 (2006) A542–A544.
[13] X.B. Huang, X. Li, H.Y. Wang, Z.L. Pan, M.Z. Qu, Z.L. Yu, Electrochim. Acta 55 (2010) 7362–7366.

[14] L.-M. Li, H.-J. Guo, X.-H. Li, Z.-X. Wang, W.-J. Peng, K.-X. Xiang, X. Cao, J. Power Sources 189 (2009) 45–50.
[15] C. Deng, S. Zhang, B.L. Fu, S.Y. Yang, L. Ma, Mater. Chem. Phys. 120 (2010) 14–17.
[16] S. Zhang, C. Deng, S.Y. Yang, Electrochem, Solid-State Lett. 12 (2009) A136–A139.
[17] R. Dominko, D.E. Conte, D. Hanzel, M. Gaberscek, J. Jamnik, J. Power Sources 178 (2008) 842–847.
[18] Z.L. Gong, Y.X. Li, G.N. He, J. Li, Y. Yang, Electrochem. Solid-State Lett. 11 (2008) A60–A63.
[19] I. Taniguchi, N. Fukuda, M. Konarova, Powder Technol. 181 (2008) 228–236.
[20] T.N.L. Doan, I. Taniguchi, J. Power Sources 196 (2011) 1399–1408.
[21] S.-I. Nishimura, S. Hayase, R. Kanno, M. Yashima, N. Nakayama, A. Yamada, J. Am. Chem. Soc. 130 (2008) 13212–13213.